DREO CR 1999-034

PRIOR Document No. : 95-0038-K(F)

FINAL REPORT

RADAR PROPAGATION AND SIGNATURE ANALYSIS FOR MARITIME ENGAGEMENT SCENARIO ANTISHIP MISSILE SIMULATIONS

ISSUE: 3.0 March 30, 1995

CONTRACT NO. : W7714-4-0177

SUPPLY ARRANGEMENT: 660ER-2-0001/I4-ER

Prepared by: Greg Carleton
Gregory Carleton
Software Engineer

Approved by: B P Rousseau
Barbara Rousseau
Quality Assurance

Approved by:
John Croft
Vice President, Defence

PRIOR Data Sciences Ltd.
240 Michael Cowpland Dr.
Kanata, Ontario
K2M 1P6
Tel: (613) 591-7235

REVISION NOTES

ISSUE	DATE	DESCRIPTION
1	1995 Jan. 18	Draft Version 1.0
2	1995 Mar. 2	Draft Version 1.2
3	1995 Mar. 29	Final Version 3.0

105-03446/

EXECUTIVE SUMMARY

The first part of this report describes the regeneration of DREO supplied ship radar cross section (RCS) data with lookup tables. Lookup tables are used to store raw RCS, smoothed RCS and scintillation data of a ship RCS. In the second part of the report, sea clutter models were examined and a method of generating clutter maps is described. The effects of phase interference (glint and scintillation), multipath, and meteorological effects on radar propagation for one way paths, relevant to the software simulation, were investigated. Sea clutter was found to most frequently follow a log-normal or Rayleigh probability distribution, depending on sea state, radar wavelength and grazing angle. An efficient method of generating numerous statistical distributions for clutter is introduced. This algorithm along with the clutter map process, allows the user to alter weather, multipath and target data as discrete cells, over the entire radar coverage zone.

TABLE OF CONTENTS

1 SCOPE 1-1
1.1 Document Overview 1-1
1.2 Relationship to Other Documents 1-1

2 REFERENCES 2-1
2.1 List of Acronyms 2-2

3 PROCESSING AND STORAGE OF RADAR CROSS SECTIONS 3-1
3.1 Introduction 3-1
3.2 Creating Lookup Tables for Raw RCS Data 3-1
3.3 Creating Lookup Tables for Low Pass Filtered RCS Data 3-3
3.4 Creating Lookup Tables for High Pass Filtered RCS Data 3-5

4 SIMULATING OF SEA CLUTTER WITH STATISTICAL MODELS 4-1
4.1 Components of Sea Clutter 4-1
4.1.1 Clutter and Spatial Correlation 4-1
4.1.2 Probability Density Function of Sea Clutter 4-2
4.2 Generation of Dynamic Clutter Map 4-3
4.2.1 Overview of Dynamic Clutter Map 4-3
4.3 Conclusion 4-7

5 ANALYSIS OF A ONE-WAY PROPAGATION MODEL 5-1
5.1 Introduction 5-1
5.1.1 Assumptions 5-1
5.2 Analysis of Multipath Interaction 5-1
5.2.1 Fading 5-1
5.2.2 Special Cases For Fading and Reinforcement of Echoes 5-2
5.2.3 Second-Time-Around Pulses and Maximum Unambiguous Range 5-2
5.2.4 Case Where Multipath Echoes Are Between True LOS Echoes 5-2
5.2.5 Case Where Multipath Echoes Partially Overlap True LOS Echoes 5-2
5.2.6 Ground Reflection 5-3
5.2.7 Variation With Grazing Angle 5-4
5.3 Simulation Case 5-5
5.4 Simulation results 5-6
5.5 Conclusion 5-6

6 FACTORS AFFECTING PROPAGATION OF RADAR SIGNALS 6-1
6.1 Introduction 6-1
6.2 Effects of Glint 6-1
6.2.1 Non-Gaussian Character of Glint Noise 6-1
6.3 Effects of Multipath 6-3

6.3.1 Effects of Meteorological Conditions 6-3
6.3.1.1 Rain Backscatter 6-3
6.3.1.2 Rain Effects 6-4
6.3.1.3 Wind Effects 6-4
6.4 Conclusion 6-4

7 IMPLEMENTATION OF RADAR CROSS SECTION, AND CLUTTER MAP-PROPAGATION MODEL INTO SIMULATION 7-1
7.1 Regeneration of Radar Cross Section 7-1
7.1.1 Regeneration of Low Pass Filtered Radar Cross Section 7-1
7.1.2 Regeneration of Scintillation of Radar Cross Section 7-2
7.1.3 Sample Probability Density Function of RCS 7-2
7.2 Creation of Clutter Map and Propagation Model 7-2
7.2.1 Introduction 7-2
7.2.2 Developing the Clutter Map Data Sets 7-3
7.3 Application of Clutter Map and Propagation Model 7-5

8 CONCLUSION 8-1

LIST OF FIGURES

Figure Page

Figure 3-1 The Raw RCS of Ship Supplied in File 'Cathin.dat' 3-2
Figure 3-2 Smoothed RCS of Ship Data Supplied in 'Cathin.dat' 3-4
Figure 3-3 Scintillation Component of Ship RCS from Data File 'Cathin.dat' 3-6
Figure 4-1 Matrix of cells describing the meteorological conditions and propagation parameters over the ocean's surface 4-4
Figure 5-1 Multipath Geometry for Low-angle Radar Tracking Scenario for Case of Flat Earth Model 5-3
Figure 5-2 Multipath Interference for supersonic sea skimmer at 8GHz. 5-7
Figure 5-3 Single Multipath Interference Pattern for Supersonic Sea-skimmer Approaching Ship. Radar frequency 18 GHz. 5-8
Figure 7-1 Position of Ship and Missile on a Matrix Structured Clutter Map 7-5
Figure 7-2 Cells can be clustered and given identical parameter values if unequal regions desired 7-6

LIST OF TABLES

Table Page

4-1 Various probability density functions 4-6

LIST OF APPENDICES

Appendix Page

Appendix A -MATLAB Simulation Software Listings A-1

1 SCOPE

1.1 Document Overview

There are two main components in this study, namely the evaluation of methods to store radar cross section (RCS) information, and the analysis of one-way radar wave propagation in a maritime environment. Radar scatter data is categorized into smoothed components and scintillation. DREO supplied ship RCS data is stored in raw RCS form, smoothed form and as scintillation, in lookup tables.

Various statistical clutter models are described for developing sea clutter maps over the line-of-sight (LOS) distance between the threat and ship. A numerical evaluation of LOS and single multipath one way radar phase interference is presented, indicating the sensitivity of wavelength to multipath cancellation.

1.2 Relationship to Other Documents

This report is a deliverable item for Phase 2 of the Maritime Engagement Scenario Antiship Missile Simulation. Previous work related to this topic was documented in NAAWS reports at DREO, along with the simulation software *NAAWS3*.

2 REFERENCES

[1] Eaves, J. L. , Reedy, E. K., *'Principles of Modern Radar'*, Van Nostrand Reinhold Co., New York, NY

[2] Wehner, D.R., *'High Resolution Radar'*, Artech House, Boston MA

[3] Skolnik, M.I., *'Introduction to Radar Systems'*, Second Ed., McGraw-Hill Book Co., New York, NY, 1980

[4] Bouche, D.P., Molinet, F.A., Mittra, R., *'Asymptotic and Hybrid Techniques for Electromagnetic Scattering'*, pp. 1658-1686, Proc. of the IEEE, Vol. 81, No. 12, Dec. 1993

[5] *'Special Issue on Radar Cross Sections of Complex Objects'*, pp. 639-823, Proc. of the IEEE, Vol. 77, No. 5, May 1989

[6] Hewer, G.A., Martin, R.D., Zeh, J., *'Robust Preprocessing for Kalman Filtering of Glint Noise'*, IEEE Trans. on AES, pp. 120-129, Volume AES-23, No. 1, 1987

[7] Barton, D.K., Cook, C.E., Hamilton, P., Editors, *'Radar Evaluation Handbook'*, Artech House, Boston MA, 1991

[8] Watts, S., *'Radar Detection Prediction in K-distributed Sea Clutter and Thermal Noise'*, IEEE Trans. AES, VOL. AES-23, No. 1, Jan. 1987, pp.40-45

[9] Haykin, S., Steinhardt, A.,Editors, *'Adaptive Radar Detection and Estimation'*, John Wiley & Sons, Inc. New York, NY, 1992, Chapter 7.

[10] Jonson, G.E., *'Construction of Particular Random Processes'*, pp. 270-285, Proc. IEEE, Vol. 82, No. 2, February 1994

[11] Guido,M., et al, *'Biparametric CFAR Procedures for Lognormal Clutter'*, IEEE Trans. on AES, Vol. 29, No.3, July 1993, pp. 798-809

[12] Locke, A. S., *'Guidance,'* D. Van Nostrand Co., Inc. Princeton, N.J. 1955, pp. 440-442.

2.1 List of Acronyms

LOS	line of sight
LUT	lookup tables
RCS	radar cross section
SA	scientific authority
DREO	Defence Research Establishment Ottawa
NAAWS	naval anit-air warfare simulation
pdf	probability density function

3 PROCESSING AND STORAGE OF RADAR CROSS SECTIONS

3.1 Introduction

Reproduction of ship scattering data can be performed using lookup tables (LUT). This is more efficient than using approximation techniques. The raw radar cross-section (RCS) data and RCS components, namely scintillation and mean values, are stored separately in lookup tables. Signal processing on the raw data does not have to be repeated each time when the tables are used.

3.2 Creating Lookup Tables for Raw RCS Data

The RCS data is read from the file 'cathin.dat' provided by the Scientific Authority (SA). A polar graph of the raw RCS data is shown in **Figure 3-1**. Matlab routine used is rawpolar.m. A vector array of dimension 360 stores the ship scattering data both in dB and power as a function of azimuth. In software, the array RCS_LUT would be described as:

RCS_LUT[bearing, elevation,wavelength,object_type] = RCS power at specified bearing, elevation and radar wavelength.

where bearing = 0, 1, ..., 359 (units are degrees);
elevation = 0, 1, ..., maximum elevation of supplied data. (units are degrees);
wavelength = 15, 16, ... 40 (units in mm); over frequency range of 7.5 to 20 GHz.
object_type = 1 for ship; 2 for decoy; 3 for missile; 4 for other item;

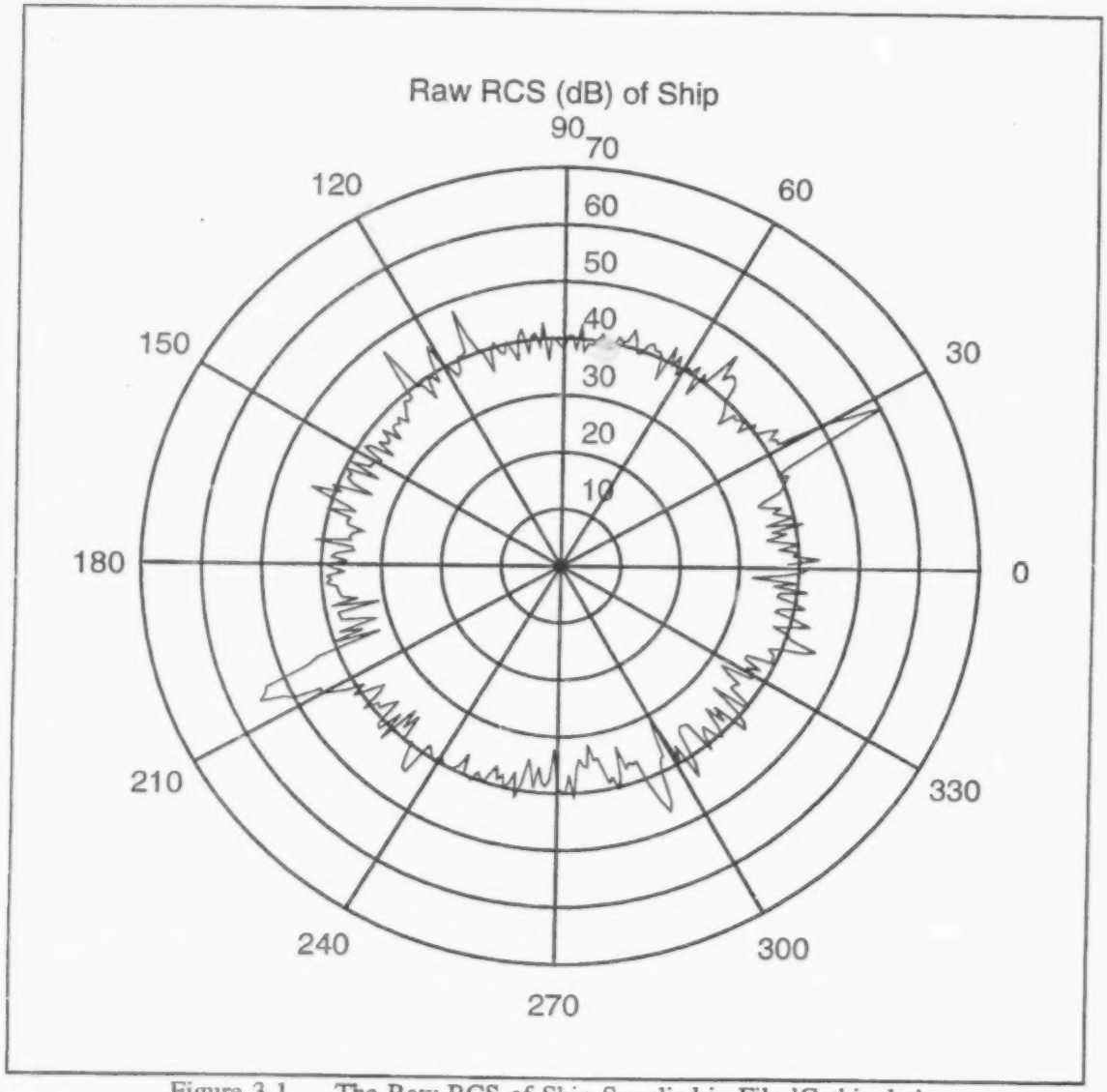

Figure 3-1 The Raw RCS of Ship Supplied in File 'Cathin.dat'

3.3 Creating Lookup Tables for Low Pass Filtered RCS Data

The low frequency components of RCS data can be derived by means of a moving average (MA) filter. The RCS power obtained from the file 'cathin.dat', is passed through this filter. Output of the MA filter contains the average RCS power, while the scintillation is attenuated. Results of the filtering are shown in **Figure 3-2**. Matlab routine used is FIR_RCS.M

$$y_i = \sum_{i=k}^{k+4} \frac{x_i}{5}$$

where y_i = filtered output for lookup table contents

and x_i = input power sample

$k=0,1,\ldots,355;$

and $i=0,1,2,\ldots,359;$ portion of LUT Addresses.

For example: If there are 360 discrete values of RCS data, covering 0° to 359°, then an array LOW_PASS_RCS_LUT of length 360 would be created. Contents of LOW_PASS_RCS_LUT would be as follows:

LOW_PASS_RCS_LUT[bearing, elevation,wavelength] = RCS power at specified bearing, elevation and radar wavelength.

where bearing = 0, 1, ..., 359 (units are degrees);
elevation = 0, 1, ..., maximum elevation of supplied data. (units are degrees);
wavelength = 15, 16, . .. 40 (units in mm); over frequency range of 7.5 to 20 GHz.
Note that for smoothed RCS data, the effects of wavelength may not be significant.

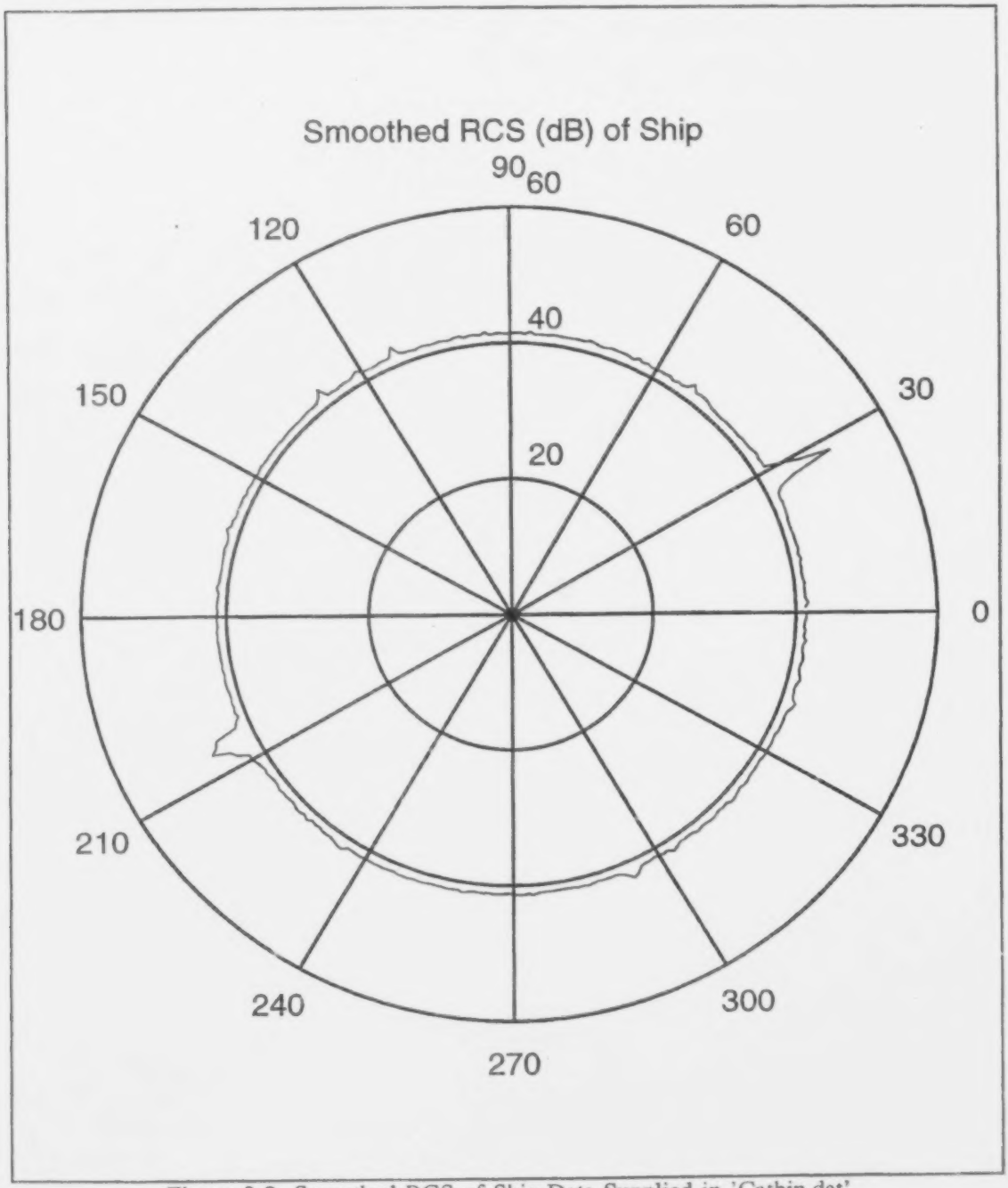

Figure 3-2 Smoothed RCS of Ship Data Supplied in 'Cathin.dat'

3.4 Creating Lookup Tables for High Pass Filtered RCS Data

Scintillation values are derived from the RCS power by high pass filtering. A differencing filter will remove any dc component and preserve all high frequency portions of the scintillation. The equation is:

$$y_i = x_i - \overline{x}_i$$

where x_i, $i = 0,1, \ldots 359$; are RCS power samples

and $\overline{x}_i$ is the local mean value of the samples

y_i = scintillation output to lookup table

Scintillation component of the ship RCS is given in **Figure 3-3**. Matlab routine used is scintrcs.m.

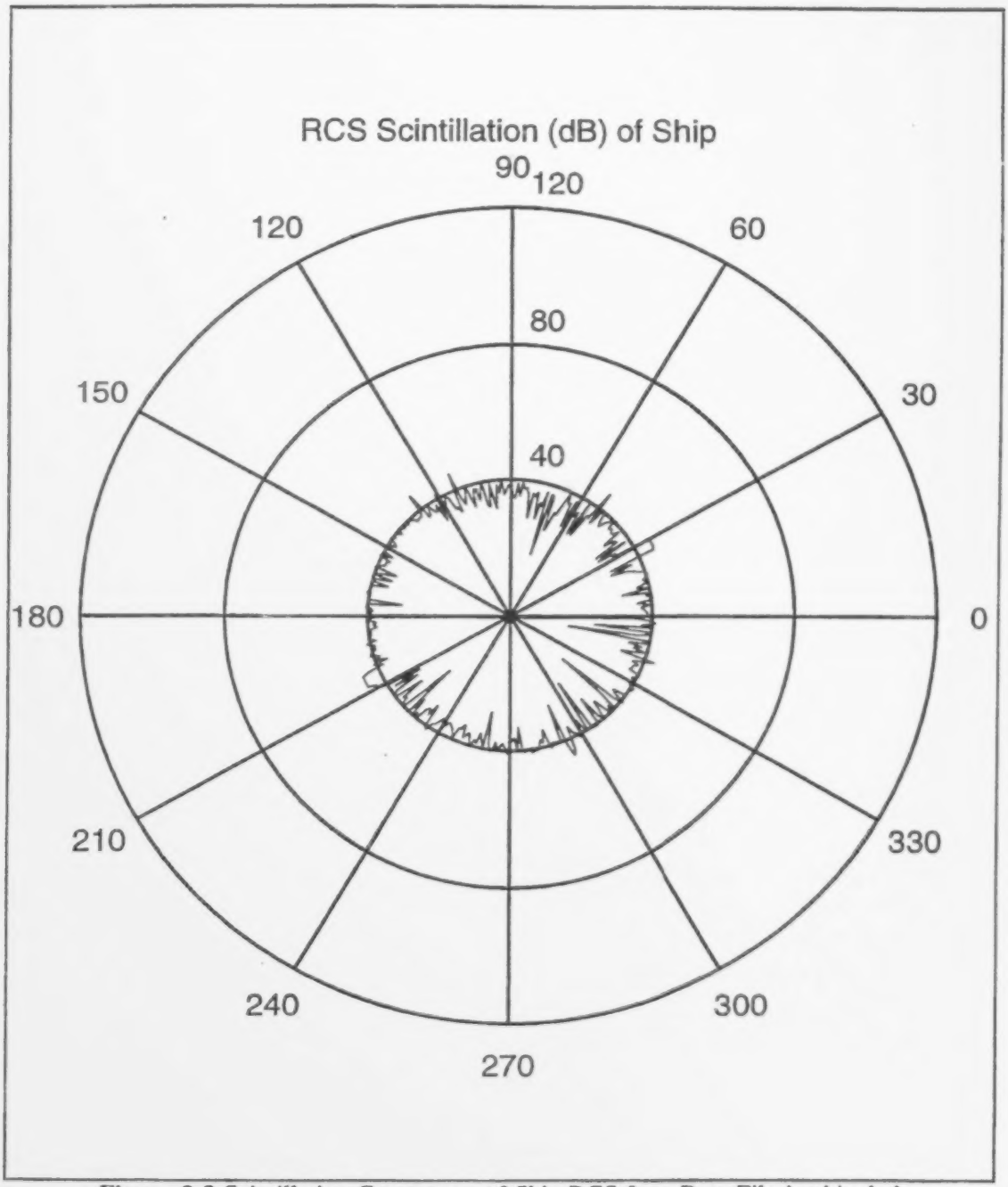

Figure 3-3 Scintillation Component of Ship RCS from Data File 'cathin.dat'

4 SIMULATING OF SEA CLUTTER WITH STATISTICAL MODELS

4.1 Components of Sea Clutter

In comparison to land clutter, sea clutter [3] exhibits larger temporal variations and smaller spatial variations. A smooth sea forward scatters all of the incident energy, so that none is reflected back toward the radar. All backscattering is due to wave and capillary action. From [7], wave height is described by means of the following quantities:

i) Sea state. The sea state is a single number that attempts to describe the characteristics of the sea surface. There is a close relationship between average wave height and wind velocity versus sea state.

ii) Average wave height. This is the mean value of the peak-to-trough height of a large number of waves.

iii) Significant wave height. The significant wave height is the average/peak-to-trough of the one-third highest waves, i. e. the height of the most prominent waves.

iv) Peak wave height. The peak wave height which is designated $h_{1/10}$ is the peak-to-trough height of the one-tenth highest waves. It has a value approximately twice the average wave height.

In general [7], sea waves are considered to be approximately sinusoidal in shape and Gaussian distributed in amplitude and period.

4.1.1 Clutter and Spatial Correlation

In the case of low grazing angles on the ocean, the time required for the sea clutter to decorrelate varies with sea state, but is cited in [3, p.484-485] as 10 ms for medium resolution X band radar. Reducing the scan period does not improve signal-to-clutter strength because of correlation between echoes on successive scans. Correlation between pulses can be modelled by sequentially adding samples from a narrowband random number generator onto unit amplitude pulses. The autocorrelation of such a weighted pulse stream would yield the correlogram representing the correlated clutter. Modelling of clutter correlation could be performed by generating a time series with accurately controlled probability density function, and correlation, to create a clutter map. With the radar as a reference point, the successive scans over a given azimuth, and varying elevation would be modelled as a sequences of one dimensional time series. The spectral components of the clutter in azimuth/elevation can be revealed by performing a 2-D Fast Fourier transform on the clutter map. Targets would be modelled as samples having specified spatial (azimuth/elevation) and amplitude (signal/noise) characteristics. Evaluation of the azimuth/elevation is sufficient to resolve the range.

4.1.2 Probability Density Function of Sea Clutter

The echo from the sea can be modeled as the results from a number of independent, random scatterers. Assuming that the contribution from each scatterer is about the same, the resulting amplitude fluctuations of the sea echo are closely modeled by a gaussian probability density function (pdf). The envelope v of such an echo at the output of the envelope detector in the radar receiver then has a Rayleigh pdf given by:

$$p(v) = \frac{2v}{\sigma^2} \exp\left(-\frac{v^2}{\sigma^2}\right)$$

where σ = *standard deviation of* v

For very high resolution radar, and at higher sea states, the clutter cross section is log normal, with a pdf of:

$$p(\sigma_c) = \frac{1}{\sqrt{2\pi}\,\sigma\,\sigma_c} \exp\left[-\frac{1}{2\sigma^2}\left(\ln\frac{\sigma_c}{\sigma_m}\right)^2\right] \qquad \sigma_c > 0$$

where σ_c = *clutter cross section*

σ_m = *median value of* σ_c

σ = *standard deviation of* $\ln \sigma_c$

The pdf describing the voltage amplitude at the output of the envelope detector, given the above clutter pdf, is:

$$p(v) = \frac{1}{\sqrt{2\pi}\,\sigma\,v} \exp\left[-\frac{1}{2\sigma^2}\left(2\ln\frac{v}{v_m}\right)^2\right]$$

where v_m *is the median value of* v

σ = *standard deviation of* $\ln \sigma_c$

In sea clutter, the Rayleigh distribution tends to underestimate the range of values obtained from real clutter, and the log-normal pdf tends to overestimate the range of variation. Other probability distributions which more closely describe certain clutter situations will be discussed.

4.2 Generation of Dynamic Clutter Map

4.2.1 Overview of Dynamic Clutter Map

The conventional clutter map is a file containing clutter power as a function of range and azimuth. Storage of clutter data for high resolution radar (e. g. < 2 °) over extensive distances (>10 km), involves enormous memory requirements, and slows down the simulation. Furthermore, the updating of the clutter map is difficult because the boundaries between meteorological clutter and wave turbulence are smeared.

An effective and efficient algorithm involves a matrix representing the clutter map, but with entries that describe large portions of the ocean's surface.

$$\begin{bmatrix} A_{11} & A_{12} & A_{13} & A_{14} & \cdots \\ A_{21} & A_{22} & A_{23} & A_{24} & \cdots \\ A_{31} & A_{32} & A_{33} & A_{34} & \cdots \\ \cdot & \cdot & \cdot & \cdot & \cdots \\ A_{N1} & A_{N2} & \cdot & \cdots & A_{NN} \end{bmatrix}$$

where each A_{ij} contains the parameters for a clutter source and propagation, namely:

i) type of distribution of clutter (based on sea state specified);
ii) initial parameters of random number generator (defining the overall clutter echo power, and variation);
iii) attenuation factor as a function of frequency and polarization, of reflected echoes;
iv) reflectivity σ^0 of the sea surface (as a function of wind vector, time duration, and grazing angle) or RCS power if cell represents an object;
v) correlation parameter ρ_{ij} between adjacent cells;
vi) radius of cell;
vii) time varying control parameter (allows time dependent variation of clutter and propagation processes); and
viii) seed number for random processes (optional, if exact repetition is required).

For example, let the threat radar be over cell $A_{1,1}$, and suppose the ship is at $A_{5,10}$. Then the radar signal will be reflected off some cell $A_{h,k}$ for low grazing angles. The weather effects in each cell lying between $A_{1,1}$ and $A_{5,10}$ will be applied to the propagating signal. Each cell A_{ij} covers an arbitrary sector of ocean surface, e. g. hexagonal segments 1 to 2 km across. These segments represent localized weather cells such as rain or snow squalls, storms, calm seas or icebergs. The situation is illustrated in **Figure 4-1**.

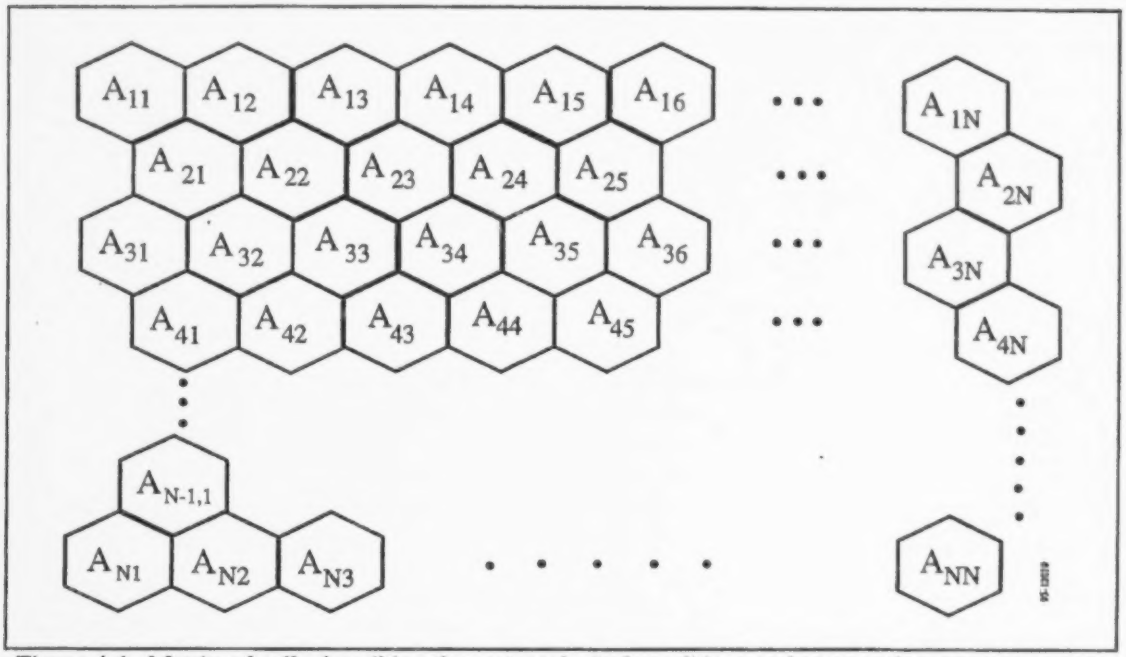

Figure 4-1 Matrix of cells describing the meteorological conditions and propagation parameters over the ocean's surface

As the radar platform and ship each move, the location of reflection varies. A pointer addresses the appropriate string of cells and evaluates the cumulative effects of propagation though each sector.

The result of a one way propagation from the ship to radar receiver through multipath and LOS would be:

$$S_{ECHO} = \sum_{i=m}^{p} \sum_{j=n}^{q} A_{ij}$$

where A_{ij} *is a function of* σ^0, ρ_{ij}, γ, *velocity, attenuation, and random distribution*

and S_{ECHO} *is the resulting echo with multipath.*

Note that using this matrix approach allows much more information to be stored about the dynamic weather processes that are occurring across the ocean's surface. Ordinary clutter maps are static and have far less descriptive information about the local atmospheric and sea activities. The clutter generators use library functions shown in **Table 4-1**, independent of the clutter map. Thus an arbitrary amount of clutter and backscatter can be generated from any particular cell. Memory is no longer a factor in simulating a time varying meteorological process over the ocean's surface. Details of the software implementation are given in Section 7.

Clutter Model	Assumptions	Benefits	Limitations
Rayleigh	clutter is homogeneous Gaussian	easy to apply to CFAR	single parameter σ controls pdf; cannot cope with heavy tailed clutter pdf,
log-normal	clutter is non-homogeneous, non-Gaussian	better pdf shape for non-Gaussian clutter than Rayleigh	two independent parameters control pdf [11]
Rician	clutter is homogeneous Gaussian	fits non-fading target with clutter [8]	sensitive to fading targets, better fit with K or log-normal
Weibull	clutter is non-homogeneous,non-Gaussian	better pdf shape for non-Gaussian clutter than Rayleigh,	two independent parameters control pdf [11]
K-distribution	clutter is correlated, and speckle exists along with Rayleigh pdf clutter, includes thermal noise effects	allows modelling of pulse-to-pulse correlation [8] better describes sea clutter than log-normal	tails affected by noise; two independent parameters control pdf [8]

Table 4-1 Various probability density functions used to represent sea clutter and meteorological backscatter for propagation conditions.

4.3 Conclusion

A number of different statistical models for clutter are presented and compared. Each distribution matches the clutter for particular conditions and under specific assumptions. In order to meet the requirements for several different sea states and various weather conditions, a clutter map which incorporates these different distributions is suggested.

Using the algorithm for a dynamic clutter map resolves the problem of modelling various clutter and propagation situations simultaneously. Under the clutter map approach, the ocean surface is displayed as a matrix, in which the user specifies the clutter and propagation characteristics within each cell. By storing function parameters in each cell that is illuminated by radar, the radar pulses are sequentially affected by propagation across all of the specified cells. The user can determine the cumulative results of various weather conditions and clutter levels before running the simulation. Since the resolution of the matrix can be made arbitrarily fine, to the limits of computer memory, the complexity of propagation and clutter conditions can be extended to closely approximate real world conditions. Each cell is time varying to model the effects of changing propagation and clutter levels as weather conditions occur.

5 ANALYSIS OF A ONE-WAY PROPAGATION MODEL

5.1 Introduction

The task, initiated by the Scientific Authority, involves the analysis and modelling of radar echoes with a single multipath component, on a pulse by pulse basis. This model contains a smooth sea, with a single multipath component and fading. Effects of multipath fading are plotted for two cases, 8 GHz and 18 GHz.

5.1.1 Assumptions

Without loss of generality, it is assumed that the radar frequency is constant, and that the sea surface is smooth. Spatial correlation may exist over portions of the illuminated target area. The ship is modelled as a specular scatterer for this simulation. Reception of the multipath is along boresight. The beam pattern is assumed to be narrow, < 5 degrees, and have negligible sidelobes. Pulse repetition frequency is assumed to be fixed. The radar frequency is set for two cases, namely 8 to 18 GHz.

5.2 Analysis of Multipath Interaction

5.2.1 Fading

In the case of a line-of-sight (LOS) echo and one multipath echo, the resultant target strength varies between zero and two, where the LOS signal strength is nominally one.

Let the LOS signal be $Ae^{j2\pi ft}$, and the multipath signal be $Be^{j2\pi f\,(t\,+\,k\Delta t)}$, where:

A = amplitude of LOS signal;
B = amplitude of multipath signal;
f = frequency of radar carrier;
t = continuous time variable;
Δt = time required to travel one half wavelength, 1/(2f) ;
T = 1/pulse repetition frequency;
t_p = pulse width;
k = integer variable.

For given Δt, we get $e^{j2\pi f(t\,+\,k\Delta t)} = e^{j2\pi ft}$ for k even, and

$$e^{j2\pi f(t\,+\,k\Delta t)} = -\,e^{j2\pi ft} \quad \text{for k odd.}$$

Δt is the period for the radar pulse to travel one half wavelength, and reach 180° phase shift. For integers K and M, the LOS pulses are received at times measured in multiples of the inter-pulse period T, namely {..., (M-1)T + $\varepsilon(t)$, MT + $\varepsilon(t)$, (M+1)T + $\varepsilon(t)$, ...} and the multipath pulses are received at times ..., (K-1)T + $\varepsilon(t)$, KT + $\varepsilon(t)$, (K+1)T + $\varepsilon(t)$, ..., where K>M, and $\varepsilon(t)$ is the remainder time function representing the one-way propagation time module T.

5.2.2 Special Cases For Fading and Reinforcement of Echoes

If $(M + K)T/\Delta t$ is an even integer, there is reinforcement between LOS and multipath.
If $(M + K)T/\Delta t$ is an odd integer, there is cancellation between LOS and multipath. For the case that A=B, then the fading causes no resultant signal.

5.2.3 Second-Time-Around Pulses and Maximum Unambiguous Range

Multipath delays echoes returning to the radar receiver. Late arrival of echoes causes range ambiguity since the multipath distance may exceed the maximum unambiguous radar range given in [1, p. 3] by $c/2f_p$, where f_p is the pulse repetition frequency in Hz and c is the speed of light. Even when the multipath distance is less than the maximum unambiguous range, the spurious echoes are a source of both range and elevation errors.

5.2.4 Case Where Multipath Echoes Are Between True LOS Echoes

For a LOS return time of MT seconds, given any positive integer N > M, the multipath return time of $(M + N)T + \alpha t_p$, for $\alpha \varepsilon [1, (T - t_p)/t_p]$, will cause a spurious echo to appear between LOS echoes, but without any overlap.

5.2.5 Case Where Multipath Echoes Partially Overlap True LOS Echoes

For a LOS return time of MT seconds, given any positive integer N > M, the multipath return time of $(M + N)T + \alpha t_p$, for $\alpha \varepsilon [-1 , 1]$, will cause a spurious echo to appear overlapped with the LOS echoes. This overlap between pulses creates errors in elevation since the centre of the echo pulse train is weighted towards the overlapped pulses. This implies that a strong echo is located at that associated elevation. In all of these multipath situations, the range gates are biased due to spurious echoes causing false ranges or exceeding the range cell resolution.

Let the LOS one way transit time be $MT + \varepsilon_{LOS}$ seconds, where $\varepsilon_{LOS} < T$, and the multipath one way transit time be $NT + \varepsilon_{MULT}$ seconds, where $\varepsilon_{MULT} < T$. Suppose the LOS signal has amplitude A and the multipath signal has amplitude B, where A>B, then the resulting signal that appears at the radar antenna is determined as follows:

$$(multipath - LOS)\ delay = T_d = (N - M)T + \epsilon_{MULT} - \epsilon_{LOS}$$

$$radar\ return = Ae^{j2\pi ft} - Be^{j2\pi(t + T_d)}$$

$$if\ |\epsilon_{MULT} - \epsilon_{LOS}| \geq 2t_p,\ then\ no\ pulse\ overlap$$

$$if\ |\epsilon_{MULT} - \epsilon_{LOS}| < 2t_p,\ then\ pulse\ overlap$$

5.2.6 Ground Reflection

Figure 5-1 [3], shows multipath geometry for low-angle radar tracking scenario for the case of a flat earth model. The ship is at height h_r above the sea surface, and the radar platform is at a distance d and height h_t. If d is very large, so that the LOS distance $R_t \approx$ multipath distance EBD, then the path difference EBD - $R_t \approx 2h_t \sin\alpha$. The angles at which maxima and minima occur, for horizontal polarization, are given in [4] as:

$$\sin\alpha = \frac{n\lambda}{4h_t} \qquad \begin{matrix} maxima\ for\ n\ odd \\ minima\ for\ n\ even \end{matrix}$$

For the first maximum to occur at a specified elevation α_1, the height of the missile radar is:

$$h_t = \frac{\lambda}{4\sin\alpha_1}$$

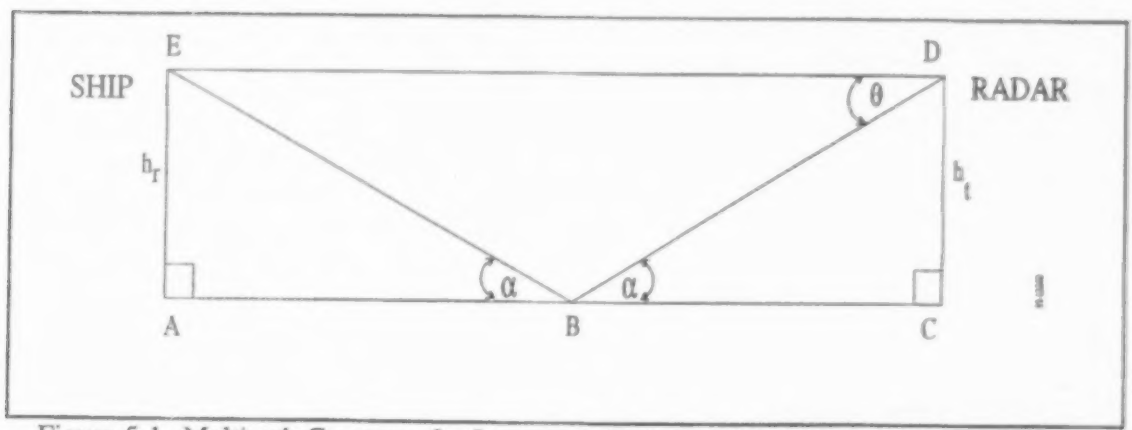

Figure 5-1 Multipath Geometry for Low-angle Radar Tracking Scenario for Case of Flat Earth Model [9]

5.2.7 Variation With Grazing Angle

From [1, p. 474], three scattering regions are identified according to the grazing angle. At near vertical incidence ($\phi \approx 90°$) the radar echo is relatively large. In this quasi-specular region, there is specular scatter from the facet like surfaces oriented perpendicular to the direction of the radar. At very low grazing angles, the clutter RCS $\sigma°$ decreases very rapidly with decreasing angle. This low angle case is the interference region in which the direct wave and the wave scattered from the sea surface are out of phase and produce destructive interference.

In [1, p. 476], the value of $\sigma°$ is generally independent of frequency for vertical polarization, except at low grazing angles. With horizontal polarization, the clutter echo decreases with decreasing frequency. This is most pronounced at the lower grazing angles. Except at grazing angles near normal incidence, the value of $\sigma°$ rises as wind speed increases.
In [7, p. 5-15], a constant γ model is given as:

$$\sigma^0 = \gamma \sin \Psi$$

where Ψ = *grazing angle at the surface*

γ = *scattering effectiveness of the surface*

This constant γ model is most accurate close to 90 degrees, but overestimates the clutter at low grazing angles. The propagation factor for paths between the radar antenna at height h and the clutter sources on the undulating, random surface of the earth can be written, for low grazing angles, as [7, p. 5-15]:

$$F_c \approx \Psi/\Psi_c + \Psi(4\pi\sigma_h/\lambda) = R_1/R$$

where σ_h =*rms surface height deviation above average*

R is range; and R_1 *is the range at which* Ψ_c *is reached*

below the critical grazing angle $\Psi_c = \lambda/4\pi\sigma_h$, *or beyond range* R_1,

the measured value $\sigma^0 F_c^4$ *should vary as* Ψ^5 *rather than* Ψ

(for small angles, $\sin\Psi \approx \Psi$)

This relationship may be modified by diffraction for large

values of σ_h

Averaging over all wind directions [7, p. 5-15], it is shown that γ depends on the Beaufort wind scale K_B and radar wavelength, such that [7, p. 5-15]:
where wavelength is in meters.

$$10\log\gamma = 6K_B - 10\log\lambda - 64$$

The rms surface deviation σ_h for wind states of 4 to 5, depends on the time and space over which the wind has acted on the sea. For steady-state conditions, the approximations are:

$$\sigma_h \approx K_B^3/300$$

$$\Psi_c \approx 24\lambda / K_B^3$$

From [7, p. 5-16], the range extent of sea clutter is determined primarily by the radar antenna height, but also by atmospheric conditions, which cause superrefraction and ducting. The horizon range can be expressed as a function of height h_r and effective earth's radius ka.

$$R_h = \sqrt{2kah_r} \approx 4130\sqrt{h_r}$$

where a = 6.5 X 10^6 m and the approximation applies to k = 4/3. with h_r and R_h in meters. Even before the horizon is reached, the declining value of

$$\sigma^0 F_c^4$$

will usually bring the clutter level below the noise level.

The velocity spectrum of sea clutter [7, p. 5-16] with a wind velocity v_w is approximately Gaussian, with a standard deviation $\sigma_v \approx v_w/8$ and a mean (downwind) between $v_w/8$ and $v_w/4$.

5.3 Simulation Case

Simulation of anti-ship missile radar detecting a ship, consists of calm sea with one multipath component. The effects of high sea states are to reduce the depth of multipath interference nulls, increase secondary multipath, increase backscatter and reduce the signal-to-noise ratio. Rain and atmospheric affects attenuate the echo, increase backscatter, and may change multipath such as by anomalous ducting. Relative power of the echo is displayed which eliminates the inverse square law of signal strength versus distance. This would be the case if the missile radar had an agc with a wide dynamic range.

5.4 Simulation results

Comparing the graphs of the 8 GHz and 18 GHz multipath cases shows the increased number of deep nulls, i. e. < -15 dB, for the 18 GHz signal. Both graphs indicated periodic peaks and nulls as a function of their respective wavelengths. See **Figures 5-2 and 5-3**. The effects of a smooth ocean surface become more pronounced as the radar wavelength becomes shorter. Conversely, with increasing sea state, the nulls for higher frequency radars tend to broaden out, as backscatter echo strength intensifies.

5.5 Conclusion

This section has described the causes of multipath fading due to destructive phase interference from a smooth ocean surface. Analytic formulas were derived for pulses, indicating the relationship between time spacing and interference. An expression for multipath as a function of grazing angle was shown. Furthermore a software model of a missile radar approaching a ship under single multipath conditions was illustrated including two graphs at radar frequencies of 8 and 18 GHz.

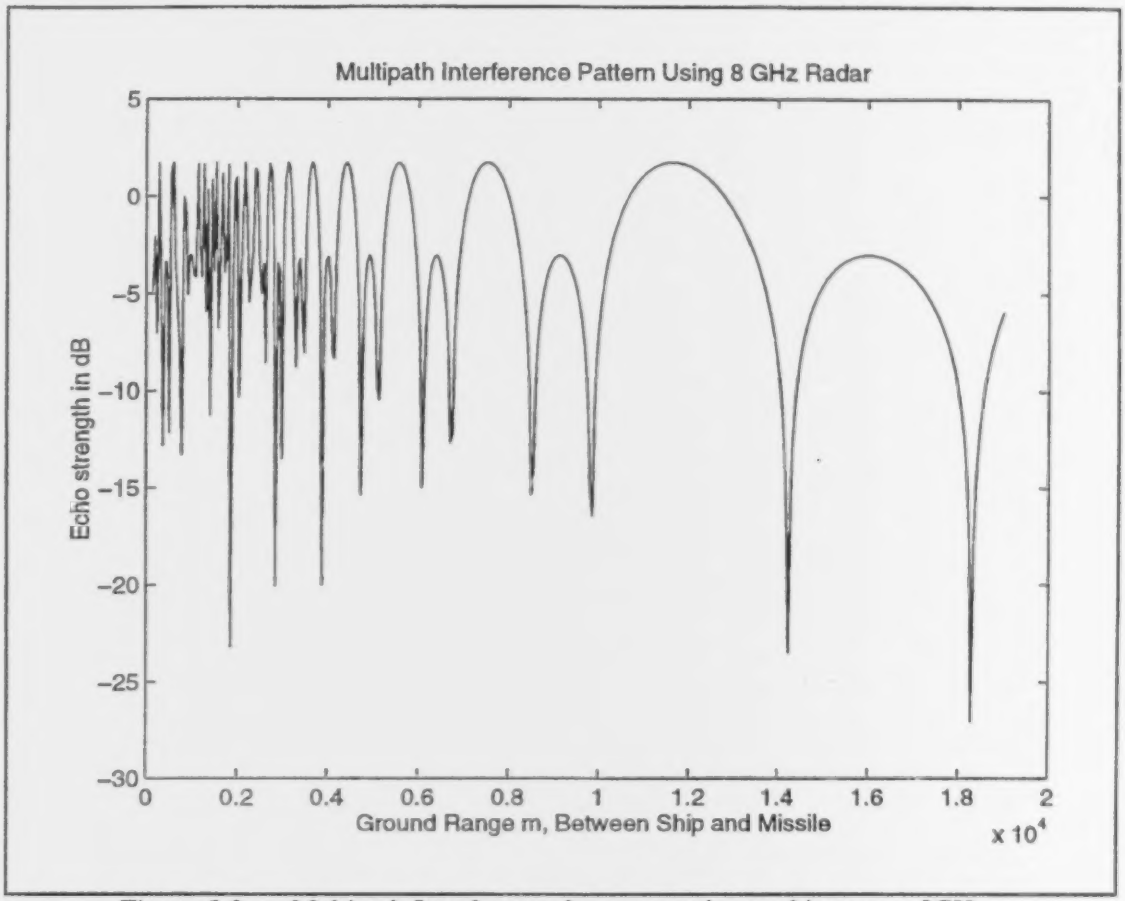

Figure 5-2 Multipath Interference for supersonic sea skimmer at 8GHz.

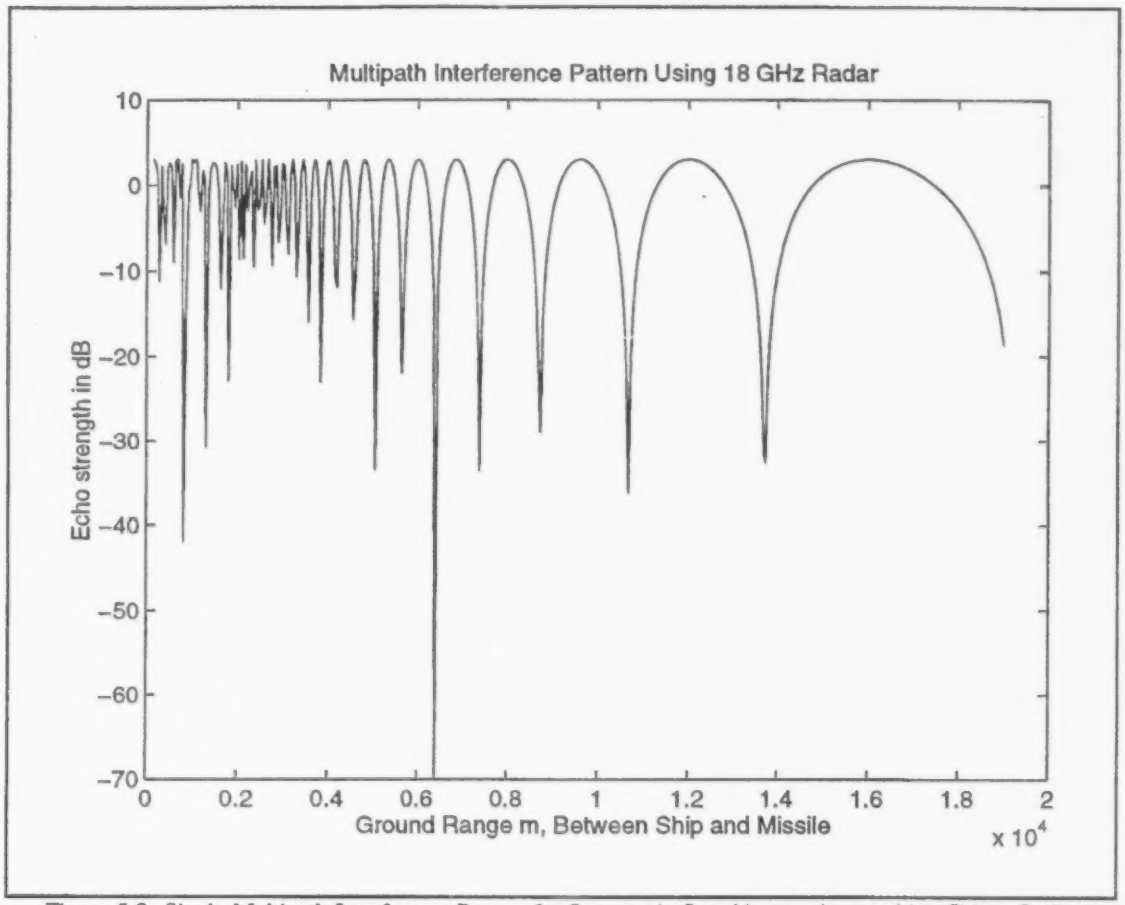

Figure 5-3 Single Multipath Interference Pattern for Supersonic Sea-skimmer Approaching Ship. Radar frequency 18 GHz.

6 FACTORS AFFECTING PROPAGATION OF RADAR SIGNALS

6.1 Introduction

The radar echo induces glint from destructive interference of target scatterers, and specular reflection. Once the echo is scattered, there is further scattering, reflection, absorption and refraction caused by the atmosphere and sea's surface. Rain absorbs and scatters radar, while the sea waves cause scattering and multipath. Wind effects the polarization of clutter and induces Doppler shift on clutter.

6.2 Effects of Glint

Changes in the target aspect with respect to the radar can cause the apparent centre of radar reflections to wander from one point to another. Generally the apparent centre of reflection might not correspond to the target centre. The random wandering of the apparent radar reflecting centre gives rise to noisy or jittered angle tracking. This form of tracking noise is called angle noise, angle scintillations, angle fluctuations, or target glint. At short range or with relatively large targets, angular fluctuations may be the chief factor limiting tracking accuracy [3]. Glint results from the radar receiving the vector sum of the echoes contributed by the individual scattering centres of a complex target, and processing it as if it were the return from a single scattering centre.

6.2.1 Non-Gaussian Character of Glint Noise

Radar signatures of complex scatterers manifest glint in the form of extremely spiky data along with a low-frequency component referred to as bright-spot wander. The bright-spot wander corresponds to the slow drift in the electromagnetic center of gravity of the target as its aspect changes. From [6], a good approximation of glint noise is:

$$Y_t = X_t + R_t$$

where R_t is a filtered Poisson process with a certain mean gap distance λ and a pulse shape $g(t)$ with a Gaussian random variable multiplier A; and X_t is a Gaussian process.

The resulting time series produces a histogram with a heavy tailed distribution. This is approximated by the Rayleigh distribution. However, for short observation times, the distribution will be spread over a wide interval due to the many outliers. Simulation of glint is possible by using the glint noise formula directly. Both Gaussian and Poisson noise generators are available as mathematical library functions. The gap between spikes can be determined from observation

of RCS plots. Gaussian statistics are the mean and variance. These can be estimated by measuring RCS plot data with the spikes removed.

i) Two Scatterer Case

A formula is derived for the glint induced error as a function of aspect angle. This can be used to estimate the glint error as the target moves. Consider [3] the simple case of two independent isotropic scatteres separated by an angular distance θ_D, as measured from the radar. This is a close approximation to the low-angle tracking problem in which the radar sees the target plus its image reflected from the surface. The relative amplitude of the two scatterers is assumed to be a, and the relative phase difference is α. Differences in phase might be due to differences in range or to reflecting properties. The ratio a is defined as a number less than unity. The angular error $\Delta\theta$ as measured from the larger of the two targets is: [12]

$$\frac{\Delta\theta}{\theta_D} = \frac{a^2 + a\cos\alpha}{1 + a^2 + 2a\cos\alpha}$$

The position of the larger of the two scatterers corresponds to $\Delta\theta/\theta_D = 0$, while the smaller-scatterer position is at $\Delta\theta/\theta_D = +1$. Positive values of $\Delta\theta$ correspond to an apparent radar center which lies between the two scatterers; negative values lie outside the target. When the echo signals from both scatterers are in phase ($\alpha = 0$), the error reduces to $a/(a + 1)$.

The tracking error $\Delta\theta$ due to glint for the two-scatterer target is directly proportional to the angular extent of the target θ_D. Since θ_D varies inversely with distance for a fixed target size, the tracking error due to glint also varies inversely with distance.

ii) Multiple Scatterer Case

In the case [3] of a large number of individual scatterers, each of the same cross section, arranged uniformly along a line of length L perpendicular to the line of sight from the radar. The resultant RCS of such a target is assumed to behave according to the Rayleigh probability distribution. Thus as the target rotates, the glint error will be Rayleigh distributed. The probability of the apparent radar center lying outside the angular region of L/R radians (in one tracking plane) is 0.134, where R is the distance to the target. Assuming the Rayleigh distribution, then 13.4 % of the time the radar will not be directed to a point on the target. Similar results for a two-dimensional model consisting of equal RCS scatterers uniformly spaced over circular area indicate that the probability that the apparent radar center lies outside this target is 0.20.

6.3 Effects of Multipath

The surface-reflected signal travels a longer path than the direct signal so that it may be possible in some cases to separate the two in time (range). The range-resolution [3] required to separate the direct from the ground-reflected signal is:

$$\Delta R = \frac{2 h_a h_t}{R}$$

where h_a = radar antenna height

h_t = target height

and R = range to the target.

Multipath creates the effect of multiple targets appearing at different elevation angles. The most important case is low angle tracking over a smooth sea surface. When the elevation angle is between 0.8 and six beamwidths, the surface reflected signal enters the radar by means of the antenna near-in sidelobes [3]. At greater ranges (elevation angles less than 0.8 beamwidths), where the antenna main beam illuminates the surface, the interference between the direct and the reflected signals can result in large errors in elevation angle. Details of phase interference and the effects of low grazing angles, including simulation results, are given in the last section.

6.3.1 Effects of Meteorological Conditions

6.3.1.1 Rain Backscatter

The backscattering properties of rain [1] depend on the transmitted frequency, the polarization, and the number and size of raindrops. Since many raindrops are approximately spherical, three scattering regimes are possible, depending on the ratio of the drop diameter to the wavelength: the Rayleigh region, where the ratio of the drop diameter D to the wavelength λ is small; the Mie region, where $D/\lambda \approx 1$; and the optical region, where D/λ is large. In the Rayleigh region, the backscatter increases rapidly with increasing frequency; in the Mie region, the backscatter varies rapidly with small changes in frequency; and in the optical region, the backscatter is independent of frequency and depends only on the cross-sectional area of the drops.

6.3.1.2 Rain Effects

A table showing rainfall rate versus backscatter cross section/unit volume is given in [1, p.501]. For most radar frequencies up to X band, rain can be approximated as Rayleigh scattering. The formula for Rayleigh cross section is given in [1, p.501, 2, p.5-17] as:

$$\eta = 7 f^4 r^{1.6} \times 10^{-12} \ m^2/m^3$$

where f = radar frequency in GHz; and
r = rainfall rate in mm/h

For purposes of the simulation, a clutter level suggested by the SA may be used instead of specifying the rainfall rate.

Attenuation due to absorption by rain is given in [2, p.2-9] as a table for two-way path attenuation with rainfall rate of 3 mm/h, over 1.3 to 240 GHz. A graphical description for rainfall rates of 0.3 to 100 mm/h over 1 to 300 GHZ is also shown.

6.3.1.3 Wind Effects

The primary effect of wind in a maritime environment is to raise the sea state. A calm sea causes the highest strength multipath due to the specular component reflected over the ocean surface. Correlation time of clutter over the sea having small wave heights is long (many tens of milliseconds, [1, p.485]). As wind velocity increases, and the winds prevail, wave heights increase, thereby creating more diffuse backscatter clutter, more low strength multipath and shorter clutter decorrelation time. At the higher microwave frequencies, Doppler shift will become more evident. This effect is noted for frequencies near the water absorption bands and winds carrying high densities of aerosols such as ice crystals.

The value of σ° increases with increasing wind speed for low grazing angles. The backscatter is quite low with winds less than about 5 knots, increases rapidly with wind speeds from about 5 to 20 knots, and increases less rapidly at higher wind speeds.

6.4 Conclusion

The main factors affecting propagation have been reviewed. Formulas and characteristics of the components of glint, multipath, meteorological effects and radar have been given. Radar wavelength and sea state are the main parameters for low grazing angles. Over long paths, the cumulative attenuation and backscatter of rain, and Doppler effects of wind become more evident.

7 IMPLEMENTATION OF RADAR CROSS SECTION, AND CLUTTER MAP-PROPAGATION MODEL INTO SIMULATION

7.1 Regeneration of Radar Cross Section

The RCS of each simulation object is initially supplied as a data file. A lookup table is used for regenerating the RCS of an object, where the object bearing, elevation and wavelength form the lookup table address of the echo power. With a file of bearing resolution is one degree.

For example: If there are 360 discrete values of RCS data, covering 0° to 359°, then an array RCS_LUT of length 360 would be created. Contents of RCS_LUT would be as follows:

RCS_LUT[bearing, elevation,wavelength,object_type] = RCS power at specified bearing, elevation and radar wavelength.

where bearing = 0, 1, ..., 359 (units are degrees);
elevation = 0, 1, ..., maximum elevation of supplied data. (units are degrees);
wavelength = 15, 16, ... 40 (units in mm); over frequency range of 7.5 to 20 GHz.
object_type = 1 for ship;
2 for decoy;
3 for missile.

7.1.1 Regeneration of Low Pass Filtered Radar Cross Section

Lookup tables for the low pass filtered version of RCS data are regenerated in the same way as unfiltered RCS data. The azimuth, elevation and wavelength are required to address the lookup table. Wavelength may not be significant for the smoothed RCS data, but it is included for consistency of structure of the lookup tables.

For example: If there are 360 discrete values of RCS data, covering 0° to 359°, then an array LOW_PASS_RCS_LUT of length 360 would be created. Contents of LOW_PASS_RCS_LUT would be as follows:

LOW_PASS_RCS_LUT[bearing, elevation,wavelength] = RCS power at specified bearing, elevation and radar wavelength.

where bearing = 0, 1, ..., 359 (units are degrees);
elevation = 0, 1, ..., maximum elevation of supplied data. (units are degrees);

wavelength = 15, 16, ... 40 (units in mm); over frequency range of 7.5 to 20 GHz.

7.1.2 Regeneration of Scintillation of Radar Cross Section

RCS scintillation data are regenerated in the same way as unfiltered RCS data. The azimuth, elevation and wavelength are required to address the lookup table.

For example: If there are 360 discrete values of RCS data, covering 0° to 359°, then an array HIGH_PASS_RCS_LUT of length 360 would be created. Contents of HIGH_PASS_RCS_LUT would be as follows:

HIGH_PASS_RCS_LUT[bearing, elevation,wavelength] = RCS power at specified bearing, elevation and radar wavelength.

where bearing = 0, 1, ..., 359 (units are degrees);
elevation = 0, 1, ..., maximum elevation of supplied data. (units are degrees);
wavelength = 15, 16, ... 40 (units in mm); over frequency range of 7.5 to 20 GHz.

7.1.3 Sample Probability Density Function of RCS

In order to obtain the probability density of an object based on RCS, several of the lookup table addresses around the aspect angle would be randomly selected. A histogram of the resulting samples will approach one of the classical probability density functions e. g. Swerling types, as the number of observations increases.

7.2 Creation of Clutter Map and Propagation Model

7.2.1 Introduction

The details of the dynamic clutter map of Section 4.2 are given here. Design of the clutter map incorporates propagation factors. Instead of storing clutter data, this map stores a matrix of parameter sequences which drive library functions. This design permits the user to model a wide range of clutter and propagation processes over the entire area of interest. As well, the matrix cells can be made to interact much as rain squalls expand and move. The level of correlation between cells is a variable which may be set initially or randomized throughout the simulation.

7.2.2 Developing the Clutter Map Data Sets

The clutter map has a structure given as follows:

$$\begin{bmatrix} A_{11} & A_{12} & A_{13} & A_{14} & \cdots \\ A_{21} & A_{22} & A_{23} & A_{24} & \cdots \\ A_{31} & A_{32} & A_{33} & A_{34} & \cdots \\ \cdot & \cdot & \cdot & \cdot & \cdots \\ A_{N1} & A_{N2} & \cdot & \cdots & A_{NN} \end{bmatrix}$$

where each A_{ij} contains the parameters for a clutter source, and propagation, namely:

i) type of distribution of clutter (based on sea state specified);
ii) initial parameters of random number generator (defining the overall clutter echo power, and variation);
iii) attenuation factor as a function of frequency and polarization, of reflected echoes;
iv) reflectivity σ^0 of the sea surface (as a function of wind vector, time duration, and grazing angle) or RCS power if cell represents an object;
v) correlation parameter ρ_{ij} between adjacent cells;
vi) radius of cell;
vii) time varying control parameter (allows time dependent variation of clutter and propagation processes); and
viii) seed number for random processes (optional, if exact repetition is required).

For example: Let A_{11}, A_{12}, and A_{13} be clutter cells and A_{23} be a cell containing a ship. The list of parameters included in A_{11}, A_{12}, and A_{13} are:

i) A_{11} will use a Rayleigh clutter distribution
A_{12} will use a Log-Normal clutter distribution
A_{13} will use a Rayleigh clutter distribution
A_{23} will use lookup tables RCS_LUT and possibly other tables with smoothed RCS data or scintillation data.

ii) A_{11} will have a mean of 2.3
A_{12} will have a mean of 3.1 and variance 14.0
A_{13} will have a mean of 2.4
A_{23} will receive the azimuth, elevation and wavelength values for

obtaining RCS values.

iii) A_{11} will have an attenuation of 0.1 db/km
A_{12} will have an attenuation of 0.15 db/km
A_{13} will have an attenuation of 0.12 db/km
A_{23} will have an attenuation of 0.1 db/km

iv) A_{11} will have a reflectivity coefficient of 0.8
A_{12} will have a reflectivity coefficient of 0.9
A_{13} will have a reflectivity coefficient of 0.8
A_{23} will use the RCS lookup tables for reflectivity.

v) A_{11} and A_{13} will have a correlation of 0.9
A_{12} and A_{11}, A_{12} and A_{13} will have a correlation of 0.7
A_{23} is not correlated with other cells, correlation is 0.0

vi) A_{11} will have a radius of 5 km
A_{12} will have a radius of 8 km
A_{13} will have a radius of 5 km
A_{23} will have a radius of 200 m.

vii) A_{11}, A_{12}, and A_{13} will be not vary with time
A_{23} will vary with time, as ship turns the RCS varies.

viii) A_{11}, A_{12}, and A_{13} will use a common seed number, e.g. 9991
A_{23} (not applicable)

7.3 Application of Clutter Map and Propagation Model

When the missile is within line of sight of the ship, a straight line is calculated joining the missile radar and ship. Secondly, a multipath line reflecting off of the ocean surface is determined, based on the user defined beam pattern and desired off-boresight lobe. The situation is illustrated in **Figure 7-1**. As the reflection point passes over each cell, the parameters stored at that point are used to invoke the clutter and propagation functions. All cells covered by the radar line are involved in propagation effects.

If the reflection occurs on cell A_{ij} then all functions related to that cell are invoked. The parameters include sea state, meteorological state and reflectivity. All other cells under the path of the radar, invoke only the parameters related to the atmosphere, since surface roughness and reflectivity are not involved. Hence for any other cell A_{kl}, all parameters such as meteorological conditions are invoked, both sea state and reflectivity are not.

Cells can be clustered to model larger regions having uniform meteorological and clutter conditions. This is shown in **Figure 7-2.**

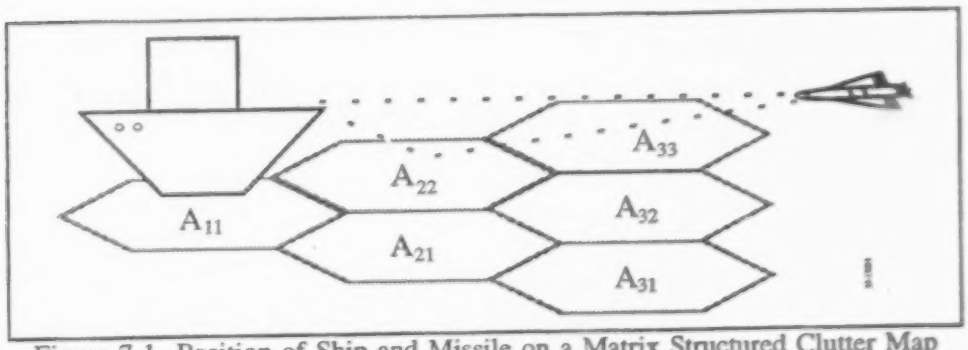

Figure 7-1 Position of Ship and Missile on a Matrix Structured Clutter Map

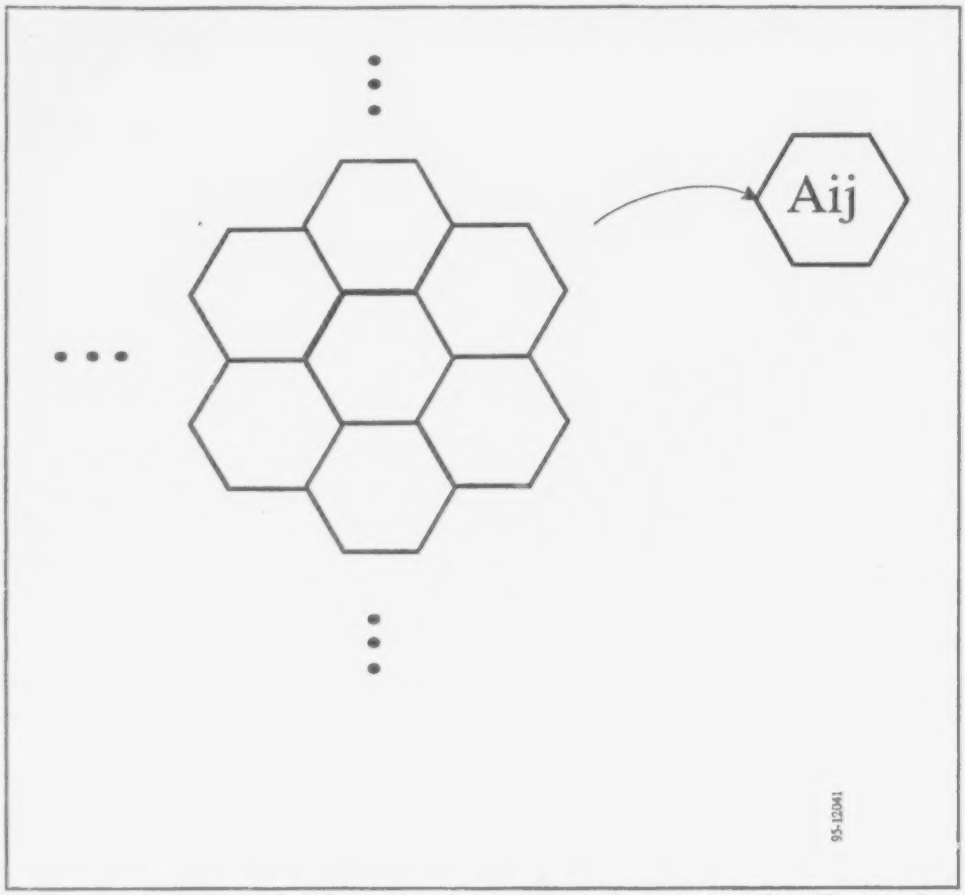

Figure 7-2 Cells can be clustered and given identical parameter values if unequal regions desired

8 CONCLUSION

This report has addressed firstly the topic of clutter simulation, with its effects on propagation, and secondly the modelling of RCS. A solution for coping with various kinds of clutter simultaneously, and under time varying conditions, has been described. The clutter map matrix technique includes propagation characteristics along with surface reflectivity, meteorological conditions and target RCS. Within the program, the user can dynamically modify the boundaries of each clutter cell, as well as altering the clutter/propagation parameters stored within.

The RCS data can be stored in the program by means of lookup tables. This permits storing the scintillation, mean level and raw RCS data separately. A sample pdf of the RCS is readily obtainable as shown in Section 7.1.3. With the modular structure available, it is convenient to replace different types of objects based on RCS data files in the simulation.

The ship or other object is now represented by a set of lookup tables. Clutter and propagation are completely described by a clutter map, with accurately known characteristics. When the user defines the receiver operating characteristics of the radar, then the entire simulation will be determined. Results will vary as a function of the statistical noise and fluctuations introduced by clutter and other processes.

APPENDIX A

MATLAB Simulation Software Listings

RAWPOLAR:

```
% RAWPOLAR produces polar plot of the raw ship RCS data
%input file is cathin.dat supplied by DREO
%open file and skip the first record

fid = open('c:\windows\cathin.dat','r');        %open the radar data file
remove_record_one = fscanf(fid,'%d',[9,1]);          %remove the first record
radar_data = fscanf(fid,'%f',[9,360]);          %contains ship RCS power and dB
relative to azimuth
transposed_data = radar_data';                  %transpose the matrix of radar data
radar_power_db = transposed_data(:,9);          %select the column containing echo
power in dB
azimuth_sequence = 2*pi:-pi/180:pi/180;         %generate a sequence over 0 to 2 pi
polar(azimuth_sequence',radar_power_db);        %plot the power on a polar graph
title('Raw RCS (dB) of Ship ');                 %put title on polar graph
```

SCINTRCS:

```
%SCINTRCS produces polar plot of the scintillation of raw ship RCS data
%input file is cathin.dat supplied by DREO
%open file and skip the first record

fid = open('c:\windows\cathin.dat','r');        %open the radar data file
remove_record_one = fscanf(fid,'%d',[9,1]);     %skip past the first record
fid2 = open('c:\matlab\rcs_mean.dat','r');      %file containing the local dc value
of RCS
radar_data = fscanf(fid,'%f',[9,360]);
%contains ship RCS power and dB relative to azimuth

dc_value = fscanf(fid2,'%f',[360,1]);

transposed_data = radar_data';
%transpose the matrix of radar data
radar_power = transposed_data(:,8);             %select the column containing echo
power
azimuth_sequence = 2*pi:-pi/180:pi/180;         %generate a sequence over 0 to 2 pi
power_buffer = radar_power;
%store radar power in a second vector
eps = 1e-12;                                    %small positive value to avoid
                                                taking log of zero
peak_power = 45;                                %threshold to limit the peak power
                                                of graph
radar_power(1) = 10*log10(abs(power_buffer(1) - dc_value(1))+eps);
                                                %perform high pass filtering by
                                                removing local mean estimate from
                                                sample value


%convert output to dB

for azimuth_index = 2:360

radar_power(azimuth_index) = 10*log10( abs(power_buffer(azimuth_index)  -
dc_value(azimuth_index))+eps );                 %for the remaining samples
if radar_power(azimuth_index) > peak_power
radar_power(azimuth_index) = peak_power;
end;

end
polar(azimuth_sequence',radar_power);
%generate a polar graph
title('RCS Scintillation (dB) of Ship ');       %include title for output
```

FIR_RCS

```
%FIR_RCS is a FIR low pass filter process for ship RCS data
%produces polar plot of the low frequency components of raw ship RCS data
%input file is cathin.dat supplied by DREO
%open file and skip the first record


fid = open('c:\windows\cathin.dat','r');                                    %open
the radar data file
remove_record_one = fscanf(fid,'%d',[9,1]);
  %skip past the first record
radar_data = fscanf(fid,'%f',[9,360]);
%contains ship RCS power and dB relative to azimuth
status =fclose(fid);
                                                                            %close
the input file after reading data
transposed_data = radar_data';
                                          %transpose the matrix of radar data
radar_power = transposed_data(:,8);
%select the column containing echo power
azimuth_sequence = 2*pi:-pi/180:pi/180;
%generate a sequence over 0 to 2 pi
filter_coefficient = 0.95;
                                          %low pass filter coefficient
eps = 1e-40;

%small positive value to avoid taking log of zero
filter_length = 10;
                                                                            %length
of moving average filter

power_buffer= 1:filter_length;
%buffer stores power samples for filtering

for i_load_data = 1:filter_length
                                          power_buffer(i_load_data) =
radar_power(1);
end;

for zero_index = 1:360, filter_output(zero_index) = 0;, end  %initialize the
                                                              lowpass filter array

for filter_index = 1:360
```

```
                                        %loop performs low pass filtering on
all RCS power samples
power_buffer(1) = radar_power(filter_index);                    %load
radar power into buffer for                    filtering

for convolve_index = 1:filter_length
filter_output(filter_index) = filter_output(filter_index) +
power_buffer(convolve_index)*(1.0/filter_length);
end
end

for power_index = 1:360
filter_output(power_index) = 10*log10(filter_output(power_index)+eps);
%convert filtered power to dB
end

polar(azimuth_sequence',filter_output');
%generate polar plot of smoothed RCS
title('Smoothed RCS (dB) of Ship ');
%insert title into polar plot
```

MULTPATH

```
% Program generates the multipath echo of missile
% approaching ship
% Signal strength is plotted in dB vs. ground range
% frequency of radar is stored as variable radar_freq_period
% reflect_point is ratio of ground distances between ship
% and reflection, and missile and reflection,  indicates the
% reflection point relative to missile is 1/2 of the total
% ground range

% ship_height is the altitude of ship above surface, for
% reflection purposes
% missile_height is the altitude of the missile
% sample_period is the period (seconds) of the sampling
% frequency
% init_launch_range is the starting distance between
% missile and ship
% missile_velocity is the velocity of missile
% radiation_velocity is the speed of light in air
% angle_of_incidence is the angle between ocean surface and
% incoming or reflected radio wave
```

```
% number_of_steps is the total number of samples taken over
% flight of missile
% range is an array storing the ground range between missile
% and ship
% depression_angle is the radar angle of elevation relative
% to the horizon
% ship_to_reflection is the distance between the ship and
% multipath reflection on ocean surface
% radar_to_reflection is the distance between the ground
% track of the missile and the reflection on the ocean
% surface

% slant_ship_reflect is the slant range between ship and
% multipath reflection
% slant_radar_reflect is the slant range between radar and
% multipath reflection
% step_index is the iteration step in the calculation
% phase_interference is an array storing the interference
% pattern caused by multipath
% line_of_sight_range is the direct distance between missile
% radar and the ship
% LOS_phase is the time delay for line of sight propagation
% multipath_phase is the time delay for multipath propagation

    reflect_point = 1.0;
    ship_height = 20;
    missile_height = 20;
    sample_period = 0.05;
    init_launch_range = 19000.0;
    ground_range = init_launch_range;
    missile_velocity = 900.0;

    radar_freq_period = 1/18e9;

    radiation_velocity = 3e8;


    number_of_steps = 420;
    range = 1:number_of_steps;
    phase_interference = 1:number_of_steps;
    for step_index = 1:number_of_steps


    ship_to_reflection = ground_range/(reflect_point + 1.0);
```

```
    radar_to_reflection = (reflect_point/(reflect_point+1.0))*ground_range;
    angle_of_incidence = atan(ship_height/ship_to_reflection);
    slant_ship_reflect = ship_to_reflection/cos(angle_of_incidence);
    slant_radar_reflect = missile_height/sin(angle_of_incidence);
    line_of_sight_range = sqrt((missile_height-ship_height)^2
+ground_range*ground_range);
    multipath_range = slant_ship_reflect + slant_radar_reflect;

    time_diff = (multipath_range - line_of_sight_range)/radiation_velocity;

    LOS_phase =
cos((2*pi/radar_freq_period)*(multipath_range/radiation_velocity));
    multipath_phase =
cos((2*pi/radar_freq_period)*(line_of_sight_range/radiation_velocity));

   phase_interference_dif =abs(LOS_phase + multipath_phase);

    range(step_index) = ground_range;
    phase_interference(step_index) = 10*log10(abs(phase_interference_dif) +
1e-35);

    ground_range = ground_range - missile_velocity*sample_period;

    end;
    plot(range,phase_interference);

    title('Multipath Interference Pattern Using 18 GHz Radar');
    xlabel('Ground Range m, Between Ship and Missile');
    ylabel('Echo strength in dB');
```

DOCUMENT CONTROL DATA

(Security classification of title, body of abstract and indexing annotation must be entered when the overall document is classified)

1. ORIGINATOR (the name and address of the organization preparing the document. Organizations for whom the document was prepared, e.g. Establishment sponsoring a contractor's report, or tasking agency, are entered in Section 8.)
Defence Research Establishment Ottawa
Ottawa, Ontario
Canada
K1A 0Z4

2. SECURITY CLASSIFICATION (overall security classification of th document including special warning terms if applicable)

UNCLASSIFIED

3. TITLE (The complete document title as indicated on the title page. Its classification should be indicated by the appropriate abbreviation (S, C or U parentheses after the title.)

Final Report: Radar Propagation and Signature Analysis for Maritime Engagement Scenerio Antiship Missile Simulations (U)

4. AUTHORS (Last name, first name, middle initial)
Carleton, Gregory

5. DATE OF PUBLICATION (month, and year of publication of document)	6a. NO. OF PAGES (total containing information. Include Annexes, Appendices, etc.)	6b. NO OF REFS (t cited in document)
30 March 1995	47	12

7. DESCRIPTIVE NOTES (category of the document, e.g. technical report, technical note or memorandum. If appropriate, enter the type of report, e. interim, progress, summary, annual or final. Give the inclusive dates when a specific reporting period is covered.)

Final Contractor Report

8. SPONSORING ACTIVITY (the name of the department project office or laboratory sponsoring the research and development, include the address.)

Defence Research Establishment Ottawa
Ottawa, Ontario, K1A 0K2

9a. PROJECT OR GRANT NO. (if appropriate, the applicable research and development project or grant number under which the document was written. Please specify whether project or grant)	9b. CONTRACT NO. (if appropriate, the applicable number under whic the document was written)
	W7714-4-0177
10a. ORIGINATOR'S DOCUMENT NUMBER (the official document number by which the document is identified by the originating activity. This number must be unique to this document.)	10b. OTHER DOCUMENT NOS. (Any other numbers which may be assigned this document either by the originator or by the sponsor)
Prior Document No. : 95-0038-K(F)	DREO CR 1999-034

11. DOCUMENT AVAILABILITY (any limitations on further dissemination of the document, other than those imposed by security classification)

- (☒) Unlimited distribution
- (☐) Distribution limited to defence departments and defence contractors; further distribution only as approved
- (☐) Distribution limited to defence departments and Canadian defence contractors; further distribution only as approved
- (☐) Distribution limited to government departments and agencies; further distribution only as approved
- (☐) Distribution limited to defence departments; further distribution only as approved
- (☐) Other (please specify):

12. DOCUMENT ANNOUNCEMENT (any limitation to the bibliographic announcement of this document. This will normally correspond to the Document Availability (1). However, where further distribution (beyond the audience specified in 11) is possible, a wider announcement audience may selected.)

Unlimited

13. ABSTRACT (a brief and factual summary of the document. It may also appear elsewhere in the body of the document itself. It is highly desirable that the abstract of classified documents be unclassified. Each paragraph of the abstract shall begin with an indication of the security classification of the information in the paragraph (unless the document itself is unclassified) represented as (S), (C), or (U). It is not necessary to include here abstracts in both official languages unless the text is bilingual).

The first part of this report describes the regeneration of DREO supplied ship radar cross section (RCS) data with lookup tables. Lookup tables are used to store raw RCS, smoothed RCS and scintillation data of a ship RCS. In the second part of the report, sea clutter models were examined and a method of generating clutter maps is described. The effects of phase interference (glint and scintillation), multipath, and meteorological effects on radar propagation for one way pathes, relevant to the software simulation, were investigated. Sea clutter was found to most frequently follow a log-normal or Rayleigh probability distribution, depending on sea state, radar wavelenght and grazing angle. An efficient method of generating numerous statistical distributions for clutter is introduced. This algorithm along with the clutter map process, allows the user to alter weather, multipath and target data as discrete cells, over the entire radar coverage zone.

14. KEYWORDS, DESCRIPTIONS or IDENTIFIERS (Technically meaningful terms or short phrases that characterize a document and could be helpful in cataloguing the document. They should be selected so that no security classification is required. Identifiers, such as equipment model designation, trade name, military project code name, geographic location may also be included. If possible keywords should be selected from a published thesaurus. e.g. Thesaurus of Engineering and Scientific Terms (TEST) and that thesaurus-identified. If it is not possible to select indexing terms which are Unclassified, the classification of each should be indicated as with the title.)

simulation
radar cross section
RCS
lookup tables
clutter maps
multipath

#510982